

# EMITTER DESIGN WITH COST-EFFECTIVE IMPLANTATION

## SUMMARY

Until very recently, ion implantation has been too expensive for PV applications. However, an ion implanter has become commercially available for PV very recently, and has been used to fabricate some devices with very low saturation current-densities. We predict possible applications utilizing a combination of implantation, annealing, device, and circuit modeling. Ion energies of 30 keV and doses in the range of  $5 \times 10^{14}$ – $1 \times 10^{15}$  cm<sup>-2</sup> are sufficient for obtaining cell efficiency levels above 20% if appropriate wafer material is used. We investigate how such emitters can be optimally used in various cell structures.

## 1. INTRODUCTION

Doping by ion implantation has been the dominant technique in the IC industry. However, until very recently, this technique has been too expensive for PV applications. Now, an ion implanter is commercially available specifically tailored to solar cells [1]. For forming emitters, rather low ion doses are necessary, which need such a short time for implantation that the mechanical handling of the wafers limits the throughput. Costs can also be saved because there is no edge isolation necessary, nor the removal of a phosphosilicate glass layer. A fairly passivating oxide can be grown during annealing.

In contrast to the IC industry, excess carrier lifetimes are of paramount importance in PV. Therefore, rapid thermal anneal (RTA), usually applied in the IC industry, is not feasible [2]. Instead, a furnace anneal is necessary with a thermal budget similar to the standard phosphorus diffusion. As there is not yet a wide range of experiments published that apply ion implantation to PV, we model favorable conditions by a combination of implantation, annealing, device, and circuit simulations.

## 2. THE MODELS

During implantation, dopant ions are introduced into the Si wafer with high energies in the range of 10's of keV. The generated crystal defects can be annealed at furnace temperatures usually employed during the standard phosphorus diffusion. It is advantageous that the ions amorphize the silicon crystal, so the subsequent annealing leads to a solid-phase epitaxial regrowth. This is easily achieved with phosphorus implantation in the energy and dose range necessary for PV. Care must be taken that amorphization also takes place with the light boron atoms, otherwise the point defects form rather stable {311} defects during annealing and lead to dislocation loops and stacking faults, which are difficult to anneal out.

An additional benefit from implantation is an acceleration of the dopant diffusion during annealing. This is so because diffusion of dopants is not possible in a perfect crystal. Instead, interstitials  $I$  and vacancies  $V$  must mediate the diffusion process. For a modern description of such mechanisms, see for example [3]. The higher the  $I$  and  $V$  densities, the faster the diffusion.

Hence, for reliable modeling, it is necessary to account for (i) the spatial distribution of point defects and dopant atoms after implantation, (ii) amorphization of Si, (iii) curing of defects during the annealing, and (iv)  $I$  and  $V$  mediated dopant diffusion. We use the software SENTAURUS PROCESS [4]. Finally, we use SENTAURUS DEVICE with the PV specific device models of Refs. [5-12] to simulate various solar cell structures with ion-

implanted emitters. With circuit modeling [13], we account for all substantial losses e.g. in the front metallization. Fig. 1 shows our reproduction of a published experiment [2]. It fits the experimental data very well, owing to the vast modeling experience in the IC industry.

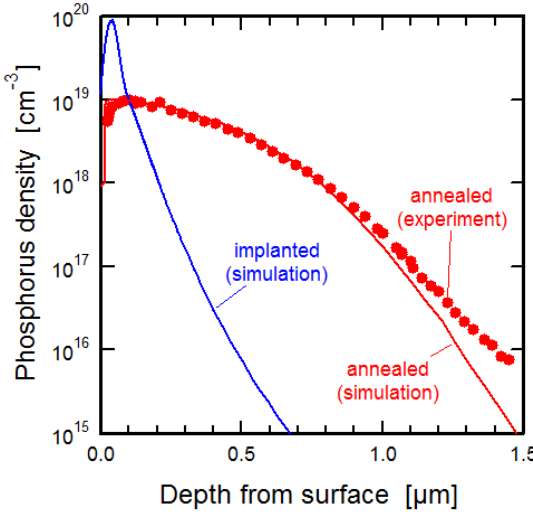


Fig. 1 Symbols: experimental phosphorus profile after implantation and annealing, see Benick et al. [2].  
Lines: our simulation.

### 3. PREDICTION OF THE DOPANT PROFILE

Figure 2 shows our prediction of various phosphorus profiles attained with the parameters listed in Table I. At the conference, we will publish experiments.

TABLE I. The implantation dose, ion energy and annealing time at 890°C in an N/O atmosphere.

Dose [cm <sup>-2</sup> ]	$5 \times 10^{14}$	$1 \times 10^{15}$
Ion energy [keV]	30	60
Annealing time [min]	20	60

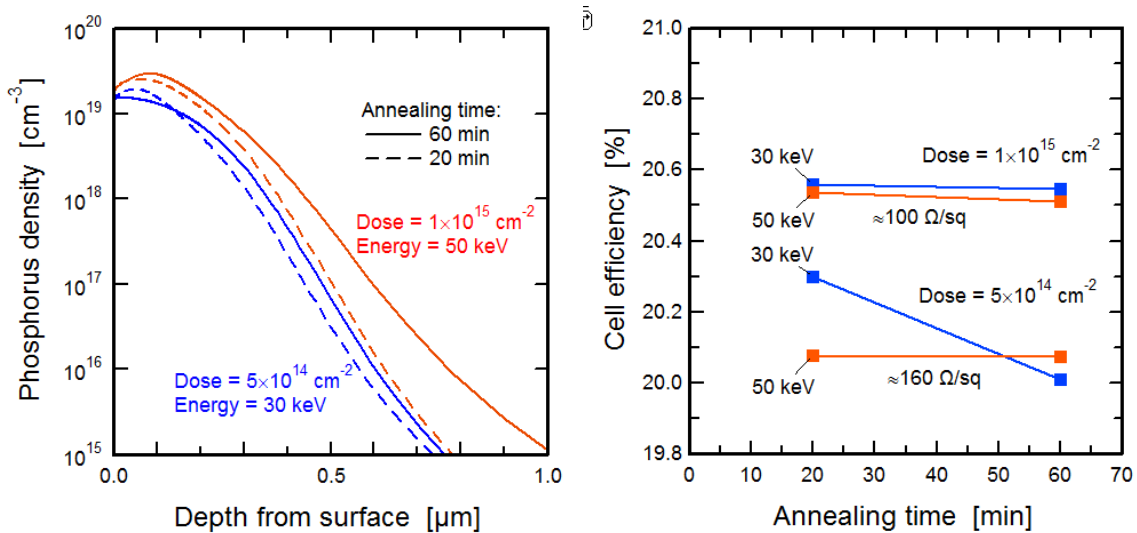


Fig. 2 Left: some simulated profiles of active phosphorus after annealing. Right: predicted cell efficiency with wafer material that has an excess carrier lifetime of 1 ms.

It is apparent from Fig. 2 that both a low surface density and a deep metallurgical junction depth can be attained with implantation. In case of a standard diffusion from the surface, long drive-in times would be necessary for achieving such emitters. It was predicted already in Ref. [14] that such emitters have the lowest saturation currents  $J_0$ .

#### 4. SOLAR CELL SIMULATION

In such phosphorus profiles, surface passivation influences  $J_0$  very strongly. For modeling, we use the values for the surface recombination velocity from Ref. [6]. If such emitters are applied to boron-doped Cz wafer material, cell efficiency is limited by SRH recombination in the base (to about 19.4% with present oxygen densities). Figure 3 therefore shows the predicted cell efficiencies in material with 1 ms lifetime. Losses due to the front metallization and a full-area BSF are accounted for. From Figure 3, it is apparent that (i) an ion energy of 30 keV is generally sufficient, (ii) the annealing time plays a role only at low doses and low energies, and (iii) the attained sheet resistivities do not put stringent conditions on the front metallization – apart from the fact that heavy doping must be used under the fingers for contacting, which can be incorporated by a shadow mask in the implanter.

- 
- [1] Varian, Gloucester, MA.
  - [2] J. Benick, N. Bateman, M. Hermle, “Very low saturation current densities on ion implanted boron emitters, 25<sup>th</sup> EU PV Solar Energy Conf. Valencia, spain, 2010, in press.
  - [3] J.D. Plummer, M.D. Deal, P.B. Griffin, “Silicon VLSI technology” (Prentice Hall, New York, 2000).
  - [4] SENTAURUS, Synopsys, Mountain View, CA.
  - [5] P.P. Altermatt, A. Schenk, F. Geelhaar, and G. Heiser, „Reassessment of the intrinsic carrier density in crystalline silicon in view of band-gap narrowing”, Journal of Applied Physics 93, 1598 (2003).
  - [6] P.P. Altermatt, J.O. Schumacher, A. Cuevas, M. J. Kerr, S.W. Glunz, R.R. King, and G. Heiser, “Numerical modeling of highly doped Si:P emitters based on Fermi–Dirac statistics and self-consistent material parameters”, Journal of Applied Physics 92, 3187 (2002).
  - [7] M. J. Kerr and A. Cuevas, “General parameterization of Auger recombination in crystalline silicon”, Journal of Applied Physics 91, 2473 (2002).
  - [8] T. Trupke, M. A. Green, P. Würfel, P. P. Altermatt, A. Wang, J. Zhao, and R. Corkish, “Temperature dependence of the radiative recombination coefficient of intrinsic crystalline silicon”, Journal of Applied Physics 94, 4930 (2003).
  - [9] K. Bothe, R. Sinton, J. Schmidt, “Fundamental Boron-Oxygen-related Carrier Lifetime Limit in Mono- and Multicrystalline Silicon”, Progress in PV 13, 287 (2005).
  - [10] J. Schmidt and A. Cuevas, „Electronic properties of light-induced recombination centers in boron-doped Czochralski silicon”, Journal of Applied Physics 86, 3175 (1999).
  - [11] S. Rein and S. W. Glunz, „Electronic properties of the metastable defect in boron-doped Czochralski silicon: Unambiguous determination by advanced lifetime spectroscopy”, Journal of Applied Physics 82, 1054 (2003).
  - [12] R. Bock, P.P. Altermatt, J. Schmidt, and R. Brendel, „Formation of aluminum–oxygen complexes in highly aluminum-doped silicon”, Semiconductor Science and Technology 25, 105007 (2010).
  - [13] P.P. Altermatt, G. Heiser, A.G. Aberle, A. Wang, J. Zhao, S.J. Robinson, S. Bowden, and M.A. Green „Spatially resolved analysis and minimization of resistive losses in high-efficiency Si solar cells”, Progress in PV 4, 399 (1996).
  - [14] A. Cuevas and M. Balbuena, “Thick-emitter silicon solar cells”, 20<sup>th</sup> IEEE Specialists Conf., Las Vegas, 1988, p.429